

Cerebral perfusion and oxygenation are impaired by folate deficiency in rat: absolute measurements with noninvasive near-infrared spectroscopy

Bertan Hallacoglu¹, Angelo Sassaroli¹, Sergio Fantini¹ and Aron M Troen^{2,3}

¹Department of Biomedical Engineering, Tufts University, Medford, Massachusetts, USA; ²Nutrition and Neurocognition Laboratory, Jean Mayer USDA Human Nutrition Research Center on Aging at Tufts University, Boston, Massachusetts, USA; ³Institute of Biochemistry, Food Science and Nutrition, Robert H Smith Faculty of Agriculture, Food and Environment, The Hebrew University of Jerusalem, Rehovot, Israel

Brain microvascular pathology is a common finding in Alzheimer's disease and other dementias. However, the extent to which microvascular abnormalities cause or contribute to cognitive impairment is unclear. Noninvasive near-infrared spectroscopy (NIRS) can address this question, but its use for clarifying the role of microvascular dysfunction in dementia has been limited due to theoretical and practical considerations. We developed a new noninvasive NIRS method to obtain quantitative, dynamic measurements of absolute brain hemoglobin concentration and oxygen saturation and used it to show significant cerebrovascular impairments in a rat model of diet-induced vascular cognitive impairment. We fed young rats folate-deficient (FD) and control diets and measured absolute brain hemoglobin and hemodynamic parameters at rest and during transient mild hypoxia and hypercapnia. With respect to control animals, FD rats featured significantly lower brain hemoglobin concentration ($72 \pm 4 \mu\text{mol/L}$ versus $95 \pm 6 \mu\text{mol/L}$) and oxygen saturation ($54\% \pm 3\%$ versus $65\% \pm 2\%$). By contrast, resting arterial oxygen saturation was the same for both groups ($96\% \pm 4\%$), indicating that decrements in brain hemoglobin oxygenation were independent of blood oxygen carrying capacity. Vasomotor reactivity in response to hypercapnia was also impaired in FD rats. Our results implicate microvascular abnormality and diminished oxygen delivery as a mechanism of cognitive impairment.

Journal of Cerebral Blood Flow & Metabolism (2011) 31, 1482–1492; doi:10.1038/jcbfm.2011.13; published online 9 March 2011

Keywords: aging; capillaries; CBF; NIRS; nutrition; VCI

Introduction

Alzheimer disease and vascular dementia are two of the most common forms of cognitive dysfunction and disability in the elderly, and their pathology frequently overlaps. Microvascular pathology, including capillary rarefaction and impaired cerebral perfusion, are a common feature of both conditions; however, the temporal and functional relation of this

postmortem pathology to in-life cognitive dysfunction and neurodegeneration are unclear (Kalaria, 2002; Kitaguchi *et al*, 2007). Nevertheless, the observed structural abnormalities provide the basis for a tenable hypothesis, implicating impaired brain perfusion and oxygen delivery as an important determinant of cognitive decline (de la Torre, 2000; Kalaria, 2002; Korczyn, 2005; Hachinski *et al*, 2006; Bell and Zlokovic, 2009; Dickstein *et al*, 2010).

Near-infrared spectroscopy (NIRS) is a noninvasive technique that can be used to address this question. It uses near-infrared light to measure tissue hemoglobin concentration and oxygen saturation, from which additional aspects of cerebrovascular function and hemodynamics may be derived. In the most common experimental paradigm, NIRS has been used to study the dynamics response of brain tissue oxy-hemoglobin ([HbO₂]) and deoxy-hemoglobin ([Hb]) concentrations to physiologic interventions such as drug treatments (Crespi *et al*, 2006), body recline (Bashir *et al*, 2006), changes in inspired

Correspondence: Dr A Troen, Nutrition and Brain Health Laboratory, Institute of Biochemistry, Food Science and Nutrition, The Robert H Smith Faculty of Agriculture, Food and Environment, The Hebrew University of Jerusalem, PO Box 12, Rehovot 76100, Israel.

E-mail: troen@agri.huji.ac.il

This work is supported by a strategic research agreement between Unilever USA and the Jean Mayer USDA Human Nutrition Research Center on Aging at Tufts, and by the US Department of Agriculture, Agricultural Research Service, under agreement No. 58-1950-7-707.

Received 15 August 2010; revised 25 January 2011; accepted 25 January 2011; published online 9 March 2011

O₂ and CO₂ (Culver *et al*, 2003), and surgical intrusions (Xia *et al*, 2007). Such studies typically provide relative measures of hemodynamic changes from baseline in response to a challenge. In some cases, the relative response is sufficient to differentiate between healthy and impaired cerebrovascular function. However, relative measurements do not fully capture potentially important parameters that might distinguish between healthy and impaired individuals, including the absolute concentration and oxygen saturation of blood hemoglobin in brain. Determining absolute hemoglobin concentrations is important because brain tissue hemoglobin concentration is a critical measure of brain–blood perfusion and determinant of oxygen delivery. As such, it may be predicted to be closely related to the microvascular pathology that is typically observed in dementia (de la Torre, 1997). Moreover, only absolute tissue hemoglobin concentrations allow for the derivation of brain microvascular blood volume. Finally, absolute measurements allow for baseline assessment, which is a more practical approach to diagnostics and monitoring of disease progression or therapeutic efficacy, and provides complementary information to that obtained from relative measurements of responses to physiologic challenges. Thus, a non-invasive, quantitative NIRS method of measuring absolute brain tissue hemoglobin concentrations and brain microvascular blood volume would significantly advance fundamental and clinical research toward understanding the role of microvascular impairments in dementia.

Although absolute brain hemoglobin concentrations have been measured using NIRS in rat, existing methods have some limitations in their accuracy, because they rely on prior wavelength calibration using a reference spectrum (Dunn *et al*, 2008), theory-based corrections to the measured absorption values (Plesnila *et al*, 2002), physiologic assumptions (Sakata *et al*, 2005), or a preliminary instrument calibration using a reference phantom (Chen *et al*, 2003). Moreover, some of these experimental methods have been moderately invasive, requiring exposure of the skull (Plesnila *et al*, 2002), or incorporation of cerebral implants (Sakata *et al*, 2005). To overcome these limitations, we developed a noninvasive multi-distance NIRS system that does not rely on any calibration procedures or estimated predefined factors. We separately measure the absorption and reduced scattering coefficients in cerebral tissue and translate the absorption coefficients at two wavelengths (690 and 830 nm) into absolute concentration and saturation of hemoglobin as shown in our recent study (Hallacoglu *et al*, 2009). The system, which incorporates a commercially available frequency-domain NIRS device and other components, and integrates them with our software, makes it possible to noninvasively, reproducibly and robustly measure hemoglobin-related parameters in anesthetized rats at rest and in response to physiologic challenges.

We applied this absolute NIRS method to our rat model of diet-induced cognitive impairment, where the impairment is thought to be due, at least in part, to brain microvascular damage in the absence of neurodegeneration. Folate deficiency and its attendant elevation of plasma homocysteine are risk factors for cognitive decline (Selhub *et al*, 2000; Kado *et al*, 2005; Troen and Rosenberg, 2005), Alzheimer's disease (Clarke *et al*, 1998), cerebrovascular disease, and stroke (Snowdon *et al*, 1997). Microvascular damage is thought to be an important potential mechanism for these associations. In mouse, consuming a diet deficient in folate and vitamins B12 and B6, has been shown to cause a 30% reduction in brain capillary density, in the absence of neurodegeneration and in association with impaired performance on tests of learning and memory (Troen *et al*, 2008b). In rats fed diets that are only deficient in folate, we found similar cognitive impairment (Troen *et al*, 2008a) and others have observed cerebral microvascular damage (Kim *et al*, 2002). Similarly, cerebrovascular reactivity is impaired in some mouse models of hyperhomocysteinemia (Dayal *et al*, 2004; Dayal and Lentz, 2008). Based on these observations, we hypothesized that folate deficiency would result in functional decrements in cerebral blood volume (CBV), oxygen delivery, and vascular reactivity, which together could account for the cognitive impairment observed in our rat model (Troen *et al*, 2008a). We ascertained these decrements by noninvasive NIRS, finding that folate-deficient (FD) rats feature absolute reductions in brain hemoglobin concentration, oxygen saturation, and abnormal dynamic responses to physiologic challenges.

Materials and methods

Rats and Diets

All animal procedures were approved by the Institutional Animal Care and Use Committee of Tufts Medical Center and Jean Mayer USDA Human Nutrition Research Center on Aging. Young male Sprague Dawley rats were systematically assigned to groups of similar mean body weight (~85 g), housed individually, and fed their assigned diet for 20 weeks. Diets formulated with AIN 93M vitamin-free ethanol-precipitated casein-based basal mix (TD 03595, Harlan Teklad, Madison, WI, USA) and an appropriate vitamin mix. The control diet (C) contained normal folate (2 mg FA/kg diet, vitamin mix TD 94047). The FD diet contained 0 mg FA/kg diet (vitamin mix TD 95052). The diets also contained 1% sulfathiazole (Sigma, St Louis, MO, USA), a nonabsorbed sulfa drug that inhibits folate formation by gut bacteria, to ensure that the animal's only source of available folate was from diet. Rats were provided with free access to water and group pair-fed in order to ensure comparable food intake by all rats (Troen *et al*, 2008a). Diets were provided for up to 20 weeks, with NIRS measurements made sequentially in a subset of rats at 10

weeks ($N=3/\text{group}$) and in all rats at 20 weeks ($N_{FD}=6$; $N_{\text{Control}}=5$).

Noninvasive Near-Infrared Spectroscopy System

Noninvasive near-infrared spectroscopy measurements were performed using a commercial frequency-domain tissue spectrometer (OxiplexTS, ISS Inc., Champaign, IL, USA) that operates at two wavelengths (690 and 830 nm) at an intensity modulation frequency of 110 MHz. Optical fibers were reproducibly positioned using a rat stereotaxic frame (Stoelting Co., Wood Dale, IL, USA), fitted with a nose mask for delivery of inhaled isoflurane anesthesia and a controlled atmosphere. One collection optical fiber bundle (3 mm in active diameter), coupled with a photomultiplier tube, was positioned at a fixed point on the posterior plane of the rat's head, ~ 4 mm behind the ear bars and ~ 1.5 mm left of the sagittal line. Two 400- μm diameter plastic clad silica illumination fibers (that guided light at 690 and 830 nm) were positioned at a distance of ~ 1 mm above the scalp to allow a drag-free linear scan and prevent coupling-based confounding. The illumination fibers were linearly scanned away from the collection fiber by means of a programmable mechanical linear stage scanning system (Velmex Inc., Bloomfield, NY, USA), at a scanning speed of 2.5 mm/s over a range of source–detector distances of ~ 5 to 12 mm, allowing for a full linear scan (back and forth) in 5 seconds, thus resulting in a 5-second acquisition time per NIRS data point for tissue hemoglobin parameters. Arterial oxygen saturation (SaO_2) was monitored independently through a veterinary pulse oximeter (Nonin, Plymouth, MN, USA) from the rat's foot during experiments. All instruments were temporally synchronized and driven through our user control interface designed in LabView software (National Instruments, Austin, TX, USA). Experimental setup and NIRS probe placement/scanning scheme are illustrated in Figure 1.

Procedures

Rats were food-deprived overnight, and their heads were shaved after brief induction of anesthesia with 3% inhaled

isoflurane. Noninvasive near-infrared spectroscopy measurements were performed in two phases consisting of intermediate (10 weeks after the initiation of diets) and final (20 weeks after the initiation of diets) measurements. For intermediate measurements, a manually controlled modified human anesthesia device was used to administer mixtures of O_2 , N_2 , and CO_2 at a constant total flow rate of 10 L/min. Following 2 minutes baseline NIRS measurements at normal fraction of inspired oxygen ($\sim 21\% \text{ FiO}_2$), 2 minutes transient hypoxia challenges ($\sim 10\% \text{ FiO}_2$) were introduced to test for system sensitivity and method development; 4 minutes normoxic recovery periods followed. By week 20, a computer-controlled GSM-3 gas mixer (CWE Inc., Ardmore, PA, USA) was incorporated for more precise control and delivery of gas mixtures at a constant total flow rate of 5 L/min. Week 20 measurements comprised the same hypoxia protocol of week 10, and in addition hypercapnia experiments that allowed evaluation of the associated hyperemic response and vasomotor reactivity (VMR). Hypercapnia experiments consisted of 1.5 minutes baseline NIRS measurements at normal fraction of inspired carbon dioxide (0% FiCO_2) followed by 3 minutes transient hypercapnia (5% FiCO_2), and 8 minutes normoxic recovery at 0% FiCO_2 . Anesthesia was maintained with 1.5% isoflurane throughout all measurements. A warming blanket was used to maintain body temperature of rats during the procedure. All procedures were repeated three times on each rat for verification of reproducibility. Coefficient of variation (i.e., s.d. divided by the mean) for repeat measurements of cerebral hemoglobin concentration and saturation was $< 3\%$.

Data Analysis

We used diffusion theory for a semi-infinite medium with extrapolated boundary conditions (Fantini *et al.*, 1994) as a model for the detected optical signal. According to this diffusion model, the changes in frequency-domain amplitude (AC) and phase (Φ) data as a function of source–detector separation are used to compute the absolute absorption (μ_a) and reduced scattering coefficients (μ_s') of the brain tissue. This method is expected to be insensitive

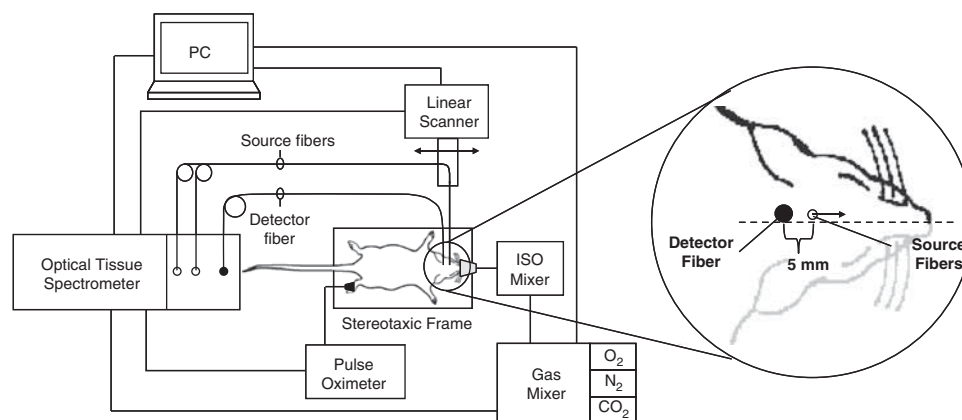


Figure 1 Experimental setup, optical fiber placement on the rat's head, and illustration of the linear scanning scheme for absolute near-infrared spectroscopy measurements.

to the superficial skin/scalp tissue layer (at least in the rat model), and does not require any calibration to cancel out unknown source/detector/optical-coupling terms. Although we collected data beginning with a source–detector separation of 5 mm, data collected at source–detector distances shorter than 8 mm were excluded from the analysis because studies on tissue-like phantoms showed that assumptions of our diffusion-based model do not hold at shorter source–detector distances (Supplementary material).

During challenge periods, we typically measured minor or no changes in reduced scattering coefficients. Figures 2A and 2B show two representative cases, in which the dashed lines represent the measured reduced scattering coefficient that are either constant (to within noise) (Figure 2A) or feature relatively minor changes (Figure 2B). Changes in opposite directions at the two wavelengths (such as the case of Figure 2B) are inconsistent with the fact that relative scattering changes in diffusive media with respect to the baseline values should not have wavelength dependence (Graaff *et al*, 1992; Kohl *et al*, 1998). Cases of observed opposite behavior of the reduced scattering coefficient at the two wavelengths are assigned to absorption/scattering crosstalk, resulting from the intrinsic ill-posedness of the inverse problem in highly scattering media. To minimize crosstalk, we set the reduced scattering coefficient to a constant (the average measured value) and recalculated absorption coefficients using such constant reduced scattering value and AC intensity data. The result of this analysis method is shown by the solid traces in Figure 2, in comparison with the dashed lines that

represent the independent measurement of both absorption and reduced scattering coefficients using AC and phase. This additional step in data analysis achieves two goals; it restores the absorption changes that are mapped onto scattering values (Figure 2D), and avoids noise contributions from phase measurements (Figures 2C and 2D).

The absorption coefficients measured at two wavelengths (690 and 830 nm) are translated into absolute $[\text{HbO}_2]$ and $[\text{Hb}]$ with a well-established method (Fantini *et al*, 1995; Hallacoglu *et al*, 2009). Using these hemoglobin parameters, we derived absolute total hemoglobin concentration ($[\text{HbT}] = [\text{HbO}_2] + [\text{Hb}]$) and oxygen saturation of hemoglobin ($\text{StO}_2 = [\text{HbO}_2]/[\text{HbT}]$) in brain tissue (Fantini *et al*, 1995). The total hemoglobin concentrations in tissue ($[\text{HbT}]$, measured with NIRS) and in blood ($[\text{HbT}]_b$, measured from blood samples) are related by the following expression (Fantini, 2002):

$$[\text{HbT}] = [\text{HbT}]_b \cdot \frac{V_b}{V_t}, \quad (1)$$

where V_b/V_t is the volume ratio of blood to tissue in the NIRS probed volume. By differentiating equation (1), one gets the following relationship between the relative changes in these parameters:

$$\frac{\Delta[\text{HbT}]}{[\text{HbT}]} = \frac{\Delta[\text{HbT}]_b}{[\text{HbT}]_b} + \frac{\Delta(V_b/V_t)}{(V_b/V_t)}, \quad (2)$$

where $\Delta(V_b/V_t)/(V_b/V_t)$ describes changes in the capillary density and in the overall crosssection of blood vessels in the investigated tissue volume. We used equation (2) to model: (1) differences between dietary groups and (2)

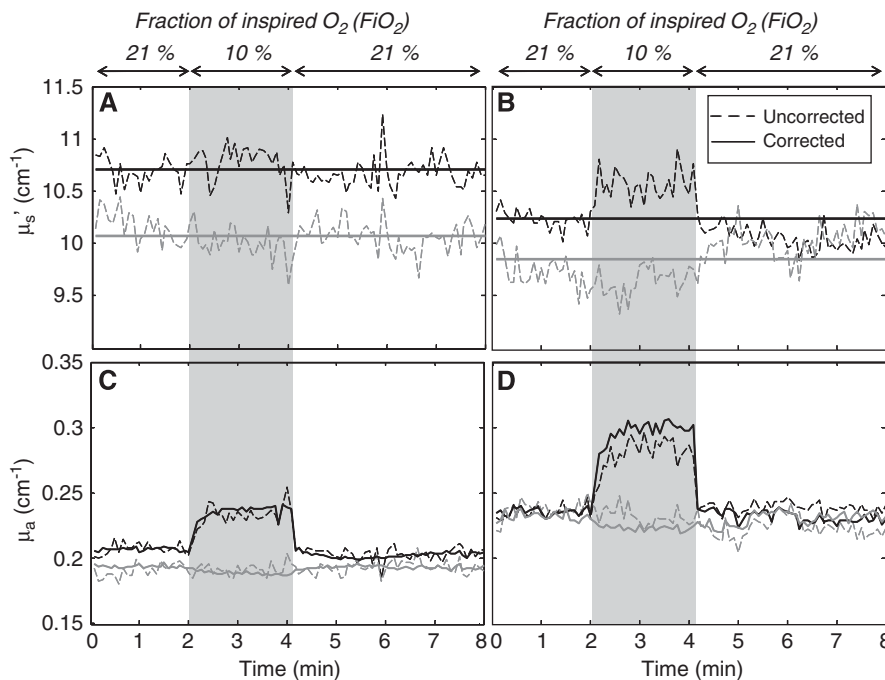


Figure 2 Reduced scattering coefficient (A, B) and absorption coefficient (C, D) of brain tissue measured in two different animals (A, C: first animal; B, D: second animal) during the hypoxia protocol. Black lines refer to a wavelength of 690 nm and gray lines to 830 nm. Dashed lines are the measurements of both optical coefficients from intensity and phase measurements (uncorrected). Solid lines are measurements from intensity only, after the reduced scattering coefficient has been set to a constant value (corrected) (average over the whole protocol).

changes in each dietary group from week 10 to week 20. Measured changes in total hemoglobin concentration ($\Delta[\text{HbT}]$) reflect only blood volume changes, and we use such relative changes as a measure of volume-related VMR, as previously reported (Vernieri *et al*, 2008):

$$\text{VMR} \equiv \frac{\Delta V_b}{V_b} = \frac{\Delta[\text{HbT}]}{[\text{HbT}]_0}, \quad (3)$$

where $[\text{HbT}]_0$ is the absolute tissue hemoglobin concentration during baseline (~ 1 minute average value) and $\Delta[\text{HbT}]$ is the change induced by hypercapnia.

We observe that a meaningful assessment of VMR does require absolute measurements so that concentration changes can be normalized to baseline values (as in equation (3)). Such absolute measurements, which are a key result of this work, are not easily achieved and in their absence one has to rely on estimating VMR without normalization to baseline values (Smielewski *et al*, 1995).

Statistical analysis for all parameters was performed using a two-tailed *t*-test with $P < 0.05$ for significance.

Hematology

Rats were euthanized after consuming diets for 20 weeks. Rats were food-deprived overnight, anesthetized with 3% inhaled isoflurane, and euthanized by exsanguination followed by perfusion through the heart with ice-cold normal saline. Complete blood counts were performed using an aliquot of ethylenediaminetetraacetic acid (EDTA) whole blood on a clinical analyzer. Plasma was separated within an hour of collection and frozen at -80°C for further analysis. Folate was measured using the Quantaphase II radioassay kit (Bio-Rad Laboratories, Hercules, CA, USA). Plasma total homocysteine was determined by HPLC (Araki and Sako, 1987).

Results

Growth

All rats gained weight on the diets and no morbidity was observed. At week 10, body weight of FD rats was not significantly different from controls (393 ± 9 g versus 410 ± 7 g; $P = 0.11$). By week 20, FD rats weighed on average 10% less than control rats (423 ± 8 g versus 467 ± 13 g; $P = 0.04$).

Hematology and Blood Chemistry

Folate-deficient diets predictably depleted plasma folate and resulted in a corresponding increase in circulating plasma total homocysteine. At 20 weeks, blood folate in FD rats was $< 10\%$ of control values (0.6 ± 0.3 ng/mL versus > 48 ng/mL (assay maximum); $P < 0.001$). In keeping with this finding, fasting plasma total homocysteine in FD rats, was more than six times higher than in controls (36.1 ± 8.2 $\mu\text{mol/L}$ versus 4.0 ± 1.2 $\mu\text{mol/L}$; $P < 0.001$). These values are consistent with findings from our previous study where measurements were conducted at 10 weeks (Troen *et al*, 2008a).

In a previous study where blood was collected at week 10, blood hemoglobin concentrations in FD rats did not differ from controls (13 ± 1 g/dL versus 13 ± 1 g/dL) (Troen *et al*, 2008a). However, by week 20 of the present study, FD rats had lower red blood cell counts (5.5 ± 1.4 cell/ μL versus $7.9 \pm 1.2 \times 10^6$ cell/ μL ; $P < 0.05$) and blood hemoglobin concentrations (11 ± 2 g/dL versus 15 ± 2 g/dL; $P < 0.05$) compared with controls. These findings are consistent with mild macrocytic anemia that is expected in chronic folate deficiency.

Near-Infrared Spectroscopy

Summary figures and tables: Figures 3 and 4 report time traces of measured parameters, namely $[\text{HbO}_2]$,

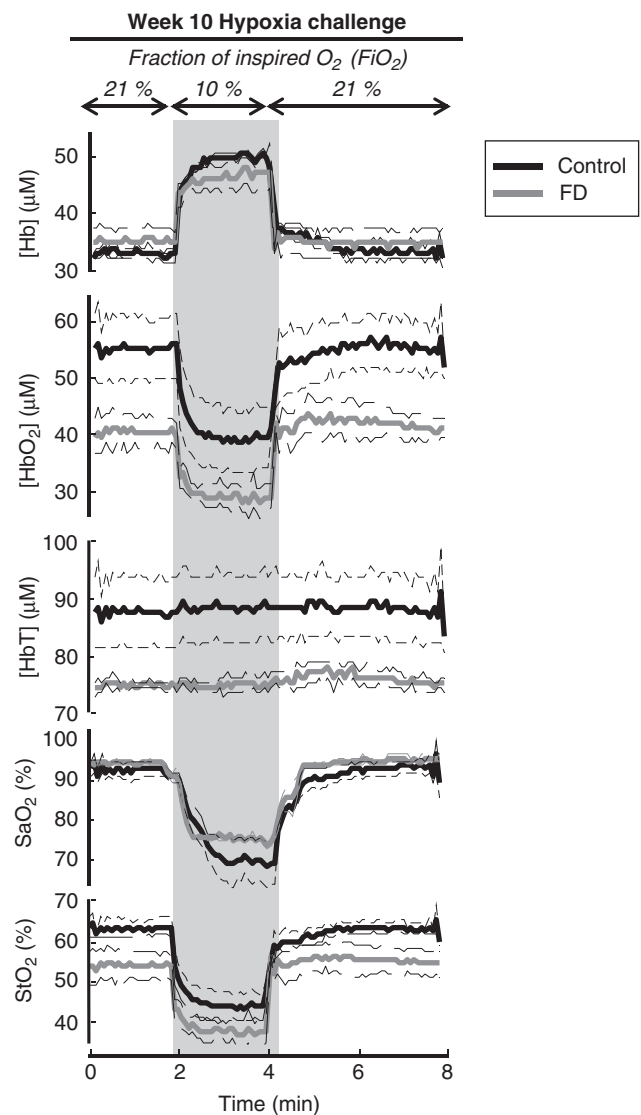


Figure 3 Time traces of tissue concentration of deoxy-hemoglobin ($[\text{Hb}]$), tissue concentration of oxy-hemoglobin ($[\text{HbO}_2]$), total hemoglobin concentration ($[\text{HbT}]$), arterial oxygen saturation (SaO_2), and tissue hemoglobin saturation (StO_2) during the hypoxia protocol 10 weeks after the start of folate-deficient (FD) diet.

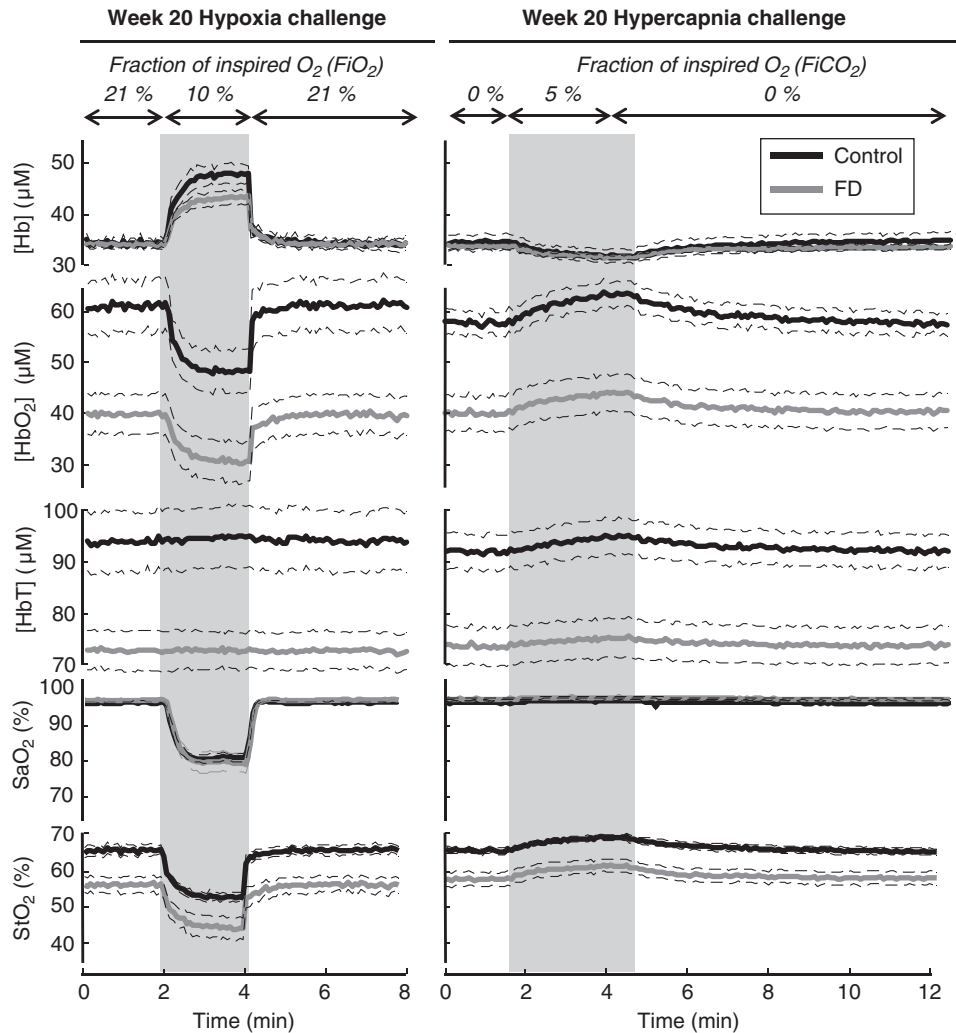


Figure 4 Time traces of tissue concentration of deoxy-hemoglobin ([Hb]), tissue concentration of oxy-hemoglobin ([HbO₂]), total hemoglobin concentration ([HbT]), arterial oxygen saturation (SaO₂), and oxygen saturation of hemoglobin (StO₂) during the hypoxia and hypercapnia protocols 20 weeks after the start of folate-deficient (FD) diet.

[Hb], and [HbT], StO₂, and SaO₂, at 10 and 20 weeks after the initiation of the diets, respectively. Solid, thick lines represent the mean values for each dietary group, whereas thin, dashed lines indicate the range corresponding to \pm one standard error from the mean. Shaded areas in Figures 3 and 4 indicate the challenge periods, and column titles denote the type of challenge (transient hypoxia or transient hypercapnia). Absolute values of the measured parameters at baseline and their changes induced by hypoxia or hypercapnia are reported in Table 1.

Baseline absolute measurements: A first striking result is the consistency of baseline values across animals within a group (control or FD), and the reproducibility of baseline values measured at week 10 and week 20. This is important considering the intrinsic challenges of noninvasive, absolute measurements of tissue hemoglobin concentrations *in vivo*. Such consistency and reproducibility of

our measurements allow us to perform meaningful comparisons among experimental groups of animals. With respect to control rats, FD rats showed comparable baseline values of [Hb] and SaO₂, and significantly lower baseline values of [HbO₂], [HbT], and StO₂ (Table 1). Baseline [HbO₂] values were lower by $17 \pm 5 \mu\text{mol/L}$ (or 31%) at week 10 and by $22 \pm 7 \mu\text{mol/L}$ (or 35%) at week 20. Baseline [HbT] values were lower by $14 \pm 5 \mu\text{mol/L}$ (or 16%) at week 10 and by $23 \pm 7 \mu\text{mol/L}$ (or 24%) at week 20. Baseline StO₂ values were lower by $11\% \pm 3\%$ (or 18%) at week 10 and by $11\% \pm 3\%$ (or 17%) at week 20 (Table 1). Changes in absolute baseline values of StO₂ and [HbT] for control and FD animals at weeks 10 and 20 are shown in Figure 5. The measured values of [HbO₂] and [HbT] are mostly associated with brain tissue, because our slope-based, frequency-domain method is insensitive to the thin ($\sim 1\text{ mm}$) superficial skin/scalp tissue layer (Franceschini *et al*, 1998). Furthermore, the specific size

Table 1 Absolute cerebral NIRS parameters measured at baseline and after induction of hypoxia or hypercapnia, in folate-deficient (FD) and control rats at 10 and 20 weeks

Hypoxia—week 10	[HbO ₂] (μmol/L)	[Hb] (μmol/L)	[HbT] (μmol/L)	StO ₂ (%)	SaO ₂ (%)
<i>Baseline</i>					
Control	54 (6)	33 (1)	87 (7)	62 (2)	92 (2)
FD	37 (3)	35 (3)	73 (1)	51 (4)	94 (6)
	Δ [HbO ₂] (μmol/L)	Δ [Hb] (μmol/L)	Δ [HbT] (μmol/L)	Δ StO ₂ (%)	Δ SaO ₂ (%)
<i>Hypoxia</i>					
Control	-17 (1)	18 (1)	0.7 (4)	-20 (2)	-19 (2)
FD	-13 (3)	13 (3)	0.1 (3)	-17 (4)	-19 (2)
Hypoxia—week 20	[HbO ₂] (μmol/L)	[Hb] (μmol/L)	[HbT] (μmol/L)	StO ₂ (%)	SaO ₂ (%)
<i>Baseline</i>					
Control	62 (5)	33 (1)	95 (6)	65 (2)	95 (3)
FD	40 (4)	33 (1)	72 (4)	54 (3)	96 (5)
	Δ [HbO ₂] (μmol/L)	Δ [Hb] (μmol/L)	Δ [HbT] (μmol/L)	Δ StO ₂ (%)	Δ SaO ₂ (%)
<i>Hypoxia</i>					
Control	-12 (1)	12 (1)	0.7 (1)	-12 (1)	-14 (1)
FD	-8 (1)	8 (1)	0.1 (3)	-11 (3)	-16 (2)
Hypercapnia—week 20	[HbO ₂] (μmol/L)	[Hb] (μmol/L)	[HbT] (μmol/L)	StO ₂ (%)	SaO ₂ (%)
<i>Baseline</i>					
Control	59 (2)	33 (2)	92 (4)	65 (1)	95 (4)
FD	41 (4)	32 (1)	72 (4)	56 (2)	96 (4)
	Δ [HbO ₂] (μmol/L)	Δ [Hb] (μmol/L)	Δ [HbT] (μmol/L)	Δ StO ₂ (%)	Δ SaO ₂ (%)
<i>Hypercapnia</i>					
Control	5.7 (7)	-2.8 (4)	2.9 (3)	4.0 (4)	0.4 (1)
FD	4.0 (5)	-2.3 (3)	1.7 (4)	4.0 (1)	0.5 (2)

[Hb], tissue concentration of deoxy-hemoglobin; [HbO₂], tissue concentration of oxy-hemoglobin; [HbT], total hemoglobin concentration in tissue; NIRS, near-infrared spectroscopy; SaO₂, arterial oxygen saturation; StO₂, oxygen saturation of hemoglobin in brain tissue. Values represent mean (s.e.m.).

and shape of each rat's head is also not expected to have a significant influence on our slope-based measurements, as we have previously showed that the surface curvature has only minor effects on the absolute measurement of the optical properties using this approach (Cerussi *et al*, 1996). Obtaining absolute tissue hemoglobin concentration [HbT] at baseline in conjunction with measured blood hemoglobin concentrations, [HbT]_b, allowed us to derive an estimate of differences between groups and changes within a group in CBV (which reflects the volume of the microvascular space) by relating blood-to-tissue partial volume according to equation (2). As shown in Figure 5, FD rats have significantly lower CBV compared with control rats at week 10, but this value appears to recover to control levels by week 20.

Percent changes induced by hypoxia: Reduction in the fraction of inspired oxygen induced percent changes in SaO₂ that were comparable (about 20%) in FD rats and control rats, while it did not induce

any detectable changes in [HbT]. In contrast with the significant differences observed between dietary groups in the absolute baseline values of [HbO₂] and StO₂ (Table 1), their percent changes induced by hypoxia were comparable in FD rats and in control rats. At week 10, percent [HbO₂] changes during hypoxia were $-35\% \pm 5\%$ in FD rats, and $-31\% \pm 4\%$ in control rats, whereas percent StO₂ changes during hypoxia were $-33\% \pm 5\%$ in FD rats, and $-32\% \pm 4\%$ in control rats. At week 20, percent [HbO₂] changes during hypoxia were $-20\% \pm 3\%$ in FD rats, and $-19\% \pm 1\%$ in control rats, whereas percent StO₂ changes during hypoxia were $-20\% \pm 3\%$ in FD rats, and $-18\% \pm 1\%$ in control rats.

Percent changes induced by hypercapnia: As shown in Figure 4, hypercapnia induced a decrease in [Hb], an increase in [HbO₂], [HbT], and StO₂, and no changes in SaO₂. The percent increases in [HbO₂], [HbT], and StO₂ induced by hypercapnia were comparable in FD and control rats. Specifically,

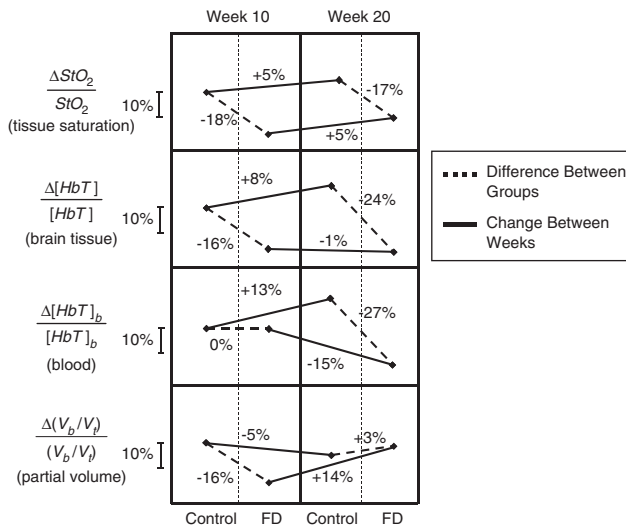


Figure 5 Summary of relative differences in cerebral tissue hemoglobin saturation (StO_2), total hemoglobin concentration in tissue ($[HbT]$), blood hemoglobin concentration ($[HbT]_b$), and partial blood volume in brain tissue (V_b/V_t) between animal groups (control and folate-deficient (FD) rats) at each time point and change within each group between weeks (week 10 and week 20 after the onset of the FD diet). It is important to note that such comparisons are only possible because of the absolute noninvasive near-infrared spectroscopy (NIRS) measurements of tissue hemoglobin concentration and saturation performed in this study.

percent increases in $[HbO_2]$ were $10\% \pm 1\%$ (FD) and $10\% \pm 1\%$ (control); percent increases in $[HbT]$ were $2.4\% \pm 0.5\%$ (FD) and $3.2\% \pm 0.4\%$ (control); percent increases in StO_2 were $7\% \pm 1\%$ (FD) and $6\% \pm 1\%$ (control). The percent decreases induced by hypercapnia in $[Hb]$ were also similar in FD rats ($7\% \pm 1\%$) and in control rats ($8\% \pm 1\%$).

The relative percent increase in $[HbT]$ was somewhat greater in control rats than in FD rats. As described in the Materials and methods—Data Analysis section, this finding indicates a greater volume-related VMR (equation (3)) in response to hypercapnia. It is possible to monitor the temporal evolution of VMR during hypercapnia by considering the time dependence of hemoglobin concentration changes. By doing that, we have derived an estimate of vasomotor responses to hypercapnia associated with volume changes (VMR, Figure 6). Slopes of the regression analysis on the first 1 minute of the hypercapnia challenge did not show statistical difference between FD and control rats in response to changes in blood volume ($P > 0.05$); however, response to these changes at the final 30 seconds of the hypercapnia challenge were significantly lower in FD than control rats ($P < 0.001$) (Figure 6).

Discussion

The ability to perform noninvasive and robust absolute measurements of cerebral tissue hemoglobin

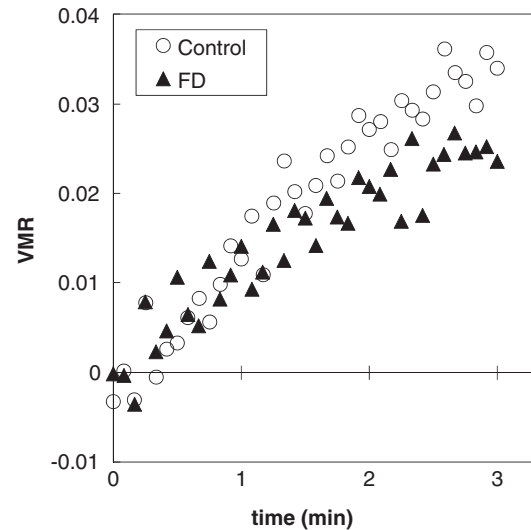


Figure 6 Vasomotor reactivity (VMR) in response to hypercapnia (time 0 is the start of a 3-minute hypercapnia period) associated with vascular volume changes). VMR is estimated from absolute near-infrared spectroscopy measurements according to equation (3). Folate-deficient (FD) rats feature a vasomotor response that is significantly dampened than the control rats by the end of the challenge period.

concentration and saturation can be of paramount importance for the characterization of hemodynamic cerebral responses as a mechanism of neurologic dysfunction.

This study shows the critical importance of obtaining absolute measurements of these parameters, as opposed to technically easier relative measurements. First, absolute measurements provide a baseline assessment that allows direct comparisons to be made between different animals, in addition to serving as a baseline reference for temporal hemodynamic responses within a given animal. In this study, absolute measurements of baseline values revealed differences between the treatment (FD) and control groups that were far more pronounced and informative than the relative hemodynamic responses of each group to hypoxia and hypercapnia. The fact that absolute measures revealed significant differences between control and treatment groups, whereas relative measures did not, shows the richer information content that absolute NIRS measures can provide for the evaluation of cerebrovascular health. Second, relative measurements typically require manipulations or physiologic challenges that may introduce additional sources of variability and may complicate the measurement protocol (e.g., the need to maintain precise levels of FiO_2 and $FiCO_2$ in the hypoxia and hypercapnia challenges considered here). Normalizing the dynamic response to a physiologic challenge to an absolute initial value can improve the accuracy and interpretability of relative dynamic measures. Combining absolute and relative values in this way allows valuable

information to be obtained, such as the derivation of VMR in equation (3).

Following this approach, we were able to show that folate deficiency can induce a significant deficit in central nervous system oxygen delivery and blood perfusion, as indicated by lower absolute tissue concentrations of [HbT] and [HbO₂], and lower tissue hemoglobin saturation (StO₂) despite normal SaO₂. This finding could explain the cognitive deficits that we have previously observed in this model (Troen *et al*, 2008a). Indeed, resting oxygen saturation (StO₂) in young FD rats was about the same as StO₂ during transient hypoxia in controls (Figure 3), suggesting that the central nervous system of FD rats might be chronically exposed to suboptimal if not overtly hypoxic conditions. Similarly, the difference in VMR between control and FD rats suggests impaired mechanisms in the regulation of cerebral blood flow during hypercapnia in FD rats. Although chronic folate deficiency causes anemia, anemia does not explain the observed cognitive or hemodynamic deficits at week 10 since blood hemoglobin is normal at week 10, and anemia only emerges later. However, anemia does contribute to the observed decrease in StO₂% and [HbT] between weeks 10 and 20. In this respect, it has been documented that mammalian physiology is well adapted to compensate for reduction in the blood hemoglobin concentration (hematocrit) through optimizing the ability of the cardiovascular system to deliver oxygen to tissues. It has been reported that these adaptive hemodynamic changes include increase in heart rate and oxygen extraction, coupled with reduction in systemic vascular resistance and mean arterial pressure (Hare, 2004; Vovenko and Chuikin, 2008).

Our results suggest that microvascular remodeling may have also occurred between weeks 10 and 20. Relative changes in partial blood volume, obtained by combining relative changes in [HbT] and [HbT]_b according to equation (2), indicate that CBV was lower in FD rats than in controls by week 10 and slightly higher than in controls by week 20 (see Figure 5). Under the assumptions of equation (2), the lower value of baseline [HbT] in FD rats versus controls at week 10 can be mostly assigned to a smaller CBV, because blood hemoglobin concentrations [HbT]_b do not differ between the groups at this time. In contrast, the lower baseline [HbT] in FD rats versus controls at week 20, can be mostly assigned to the observed reduction in [HbT]_b in the FD rats. The calculated reduction and recovery of CBV in the FD rats suggests that considerable microvascular remodeling might have occurred over the course of the study.

Intriguingly, the initial reduction in CBV that we observed at week 10 might be consistent with the findings from other studies of capillary rarefaction in mice fed B-vitamin-deficient diets for 10 weeks (Troen *et al*, 2008b) and with brain microvascular damage in rats fed FD diets for 8 weeks (Kim *et al*,

2002). Assuming that the chronic reduction of brain StO₂ observed between weeks 10 and 20 does in fact result in tissue hypoxia, one might also speculate that the subsequent recovery of CBV by week 20 could be due to a hypoxia-driven angiogenesis that has been observed physiologically (LaManna *et al*, 2004) and in neurodegenerative disease (Kalaria *et al*, 1998). Clearly, further studies will be necessary to validate our noninvasive NIRS-derived CBV estimates against anatomical measures of capillary density and through comparison with other imaging modalities. Although this remains to be accomplished, the method described here offers the opportunity to do so in this and other animal models of vascular cognitive impairment. One potential limitation of this study is the use of isoflurane for anesthesia, which can induce cerebral vasodilation and therefore might have ameliorated differences that might have otherwise be present in awake rats (Lee *et al*, 1994; Duong, 2007; Franceschini *et al*, 2010).

Conclusion

In summary, we have reported significantly lower values of baseline [HbO₂], [HbT], and StO₂ in young FD rats with respect to controls, 10 weeks after the initiation of the FD diet. This level of deficiency was maintained at week 20, even though the relative contributions from microvascular changes and anemia were found to be different at week 10 and week 20. In addition, we found that FD rats feature impaired VMR in response to hypercapnia. Measured differences in absolute values of cerebral tissue hemoglobin saturation, concentrations of hemoglobin, and vascular reactivity to inspiration challenges between FD and control rats could explain the cognitive impairment that we have previously observed in this model.

The present study has shown that diet-induced folate deficiency causes profound functional changes to brain hemodynamics and oxygen delivery in young rats. The absolute NIRS measurements reported in this work are significant, robust, and more informative than relative measurements. They allowed us to reveal functional cerebrovascular effects of folate deficiency, and provide a basis to test the hypothesis that such functional vascular changes are related to cognitive impairment. The innovative approach that we have developed allows for absolute NIRS parameters to be applied to the study of vascular cognitive impairment and cerebrovascular disease in other animal models. This in turn should facilitate the development of clinically useful NIRS measures of cerebrovascular health.

Acknowledgements

The authors thank Yang Yu for useful discussions about the hardware setup, and Debbie Chen for her

contributions to preliminary measurements. Any opinions, findings, conclusion, or recommendations expressed in this publication are those of the authors and do not necessarily reflect the view of the US Department of Agriculture.

Disclosure/conflict of interest

The authors declare no conflict of interest.

References

- Araki A, Sako Y (1987) Determination of free and total homocysteine in human plasma by high-performance liquid chromatography with fluorescence detection. *J Chromatogr* 422:43–52
- Bashir Z, Miller J, Miyan JA, Thorniley MS (2006) A near infrared spectroscopy study investigating oxygen utilisation in hydrocephalic rats. *Exp Brain Res* 175:127–38
- Bell RD, Zlokovic BV (2009) Neurovascular mechanisms and blood-brain barrier disorder in Alzheimer's disease. *Acta Neuropathol* 118:103–13
- Cerussi AE, Maier JS, Fantini S, Franceschini MA, Gratton E (1996) The frequency-domain multi-distance method in the presence of curved boundaries. In: *OSA Trends in Optics and Photonics on Biomedical Optical Spectroscopy and Diagnostics* (Muraca ES, Benaron D, eds). Optical Society of America: Orlando, FL pp 92–7
- Chen Y, Taylor DR, Intes X, Chance B (2003) Correlation between near-infrared spectroscopy and magnetic resonance imaging of rat brain oxygenation modulation. *Phys Med Biol* 48:417–27
- Clarke R, Smith AD, Jobst KA, Refsum H, Sutton L, Ueland PM (1998) Folate, vitamin B12, and serum total homocysteine levels in confirmed Alzheimer disease. *Arch Neurol* 55:1449–55
- Crespi F, Donini M, Bandera A, Congestri F, Formenti F, Sonntag V, Heidbreder C, Rovati L (2006) Near-infrared oxymeter biosensor prototype for non-invasive *in vivo* analysis of rat brain oxygenation: effects of drugs of abuse. *J Opt A Pure Appl Opt* 8:S528–34
- Culver JP, Durduran T, Cheung C, Furuya D, Greenberg JH, Yodh AG (2003) Diffuse optical measurement of hemoglobin and cerebral blood flow in rat brain during hypercapnia, hypoxia and cardiac arrest. *Adv Exp Med Biol* 510:293–7
- Dayal S, Arning E, Bottiglieri T, Boger RH, Sigmund CD, Faraci FM, Lentz SR (2004) Cerebral vascular dysfunction mediated by superoxide in hyperhomocysteinemic mice. *Stroke* 35:1957–62
- Dayal S, Lentz SR (2008) Murine models of hyperhomocysteinemia and their vascular phenotypes. *Arterioscler Thromb Vasc Biol* 28:1596–605
- de la Torre JC (1997) Hemodynamic consequences of deformed microvessels in the brain in Alzheimer's disease. *Ann N Y Acad Sci* 826:75–91
- de la Torre JC (2000) Impaired cerebrovascular perfusion. Summary of evidence in support of its causality in Alzheimer's disease. *Ann N Y Acad Sci* 924:136–52
- Dickstein DL, Walsh J, Brautigam H, Stockton SD, Jr, Gandy S, Hof PR (2010) Role of vascular risk factors and vascular dysfunction in Alzheimer's disease. *Mt Sinai J Med* 77:82–102
- Dunn JF, Zhang Q, Wu Y, Srinivasan S, Smith MR, Shaw RA (2008) Monitoring angiogenesis noninvasively with near-infrared spectroscopy. *J Biomed Opt* 13:064043
- Duong TQ (2007) Cerebral blood flow and BOLD fMRI responses to hypoxia in awake and anesthetized rats. *Brain Res* 1135:186–94
- Fantini S (2002) A haemodynamic model for the physiological interpretation of *in vivo* measurements of the concentration and oxygen saturation of haemoglobin. *Phys Med Biol* 47:N249–57
- Fantini S, Franceschini MA, Gratton E (1994) Semi-infinite-geometry boundary problem for light migration in highly scattering media: a frequency-domain study in the diffusion approximation. *J Opt Soc Am* 11:2128–38
- Fantini S, Franceschini MA, Maier JS, Walker SA, Barbieri B, Gratton E (1995) Frequency-domain multichannel optical detector for noninvasive tissue spectroscopy and oximetry. *Opt Eng* 34:32–42
- Franceschini MA, Fantini S, Paunescu LA, Maier JS, Gratton E (1998) Influence of a superficial layer in the quantitative spectroscopic study of strongly scattering media. *Appl Opt* 37:7447–58
- Franceschini MA, Radhakrishnan H, Thakur K, Wu W, Ruvinskaya S, Carp S, Boas DA (2010) The effect of different anesthetics on neurovascular coupling. *Neuroimage* 51:1367–77
- Graaff R, Aarnoudse JG, Zijp JR, Slood PMA, Demul FFM, Greve J, Koelink MH (1992) Reduced light-scattering properties for mixtures of spherical-particles—a simple approximation derived from Mie calculations. *Appl Opt* 31:1370–6
- Hachinski V, Iadecola C, Petersen RC, Breteler MM, Nyenhuis DL, Black SE, Powers WJ, DeCarli C, Merino JG, Kaloria RN, Vinters HV, Holtzman DM, Rosenberg GA, Wallin A, Dichgans M, Marler JR, Leblanc GG (2006) National Institute of Neurological Disorders and Stroke-Canadian Stroke Network vascular cognitive impairment harmonization standards. *Stroke* 37:2220–41
- Hallacoglu B, Matulewicz RS, Paltiel HJ, Padua H, Gargollo P, Cannon G, Alomari A, Sassaroli A, Fantini S (2009) Noninvasive assessment of testicular torsion in rabbits using frequency-domain near-infrared spectroscopy: prospects for pediatric urology. *J Biomed Opt* 14:054027
- Hare GM (2004) Anaemia and the brain. *Curr Opin Anaesthesiol* 17:363–9
- Kado DM, Karlamangla AS, Huang MH, Troen A, Rowe JW, Selhub J, Seeman TE (2005) Homocysteine versus the vitamins folate, B6, and B12 as predictors of cognitive function and decline in older high-functioning adults: MacArthur Studies of Successful Aging. *Am J Med* 118:161–7
- Kalaria R (2002) Similarities between Alzheimer's disease and vascular dementia. *J Neurol Sci* 203–204:29–34
- Kalaria RN, Cohen DL, Premkumar DR, Nag S, LaManna JC, Lust WD (1998) Vascular endothelial growth factor in Alzheimer's disease and experimental cerebral ischemia. *Brain Res Mol Brain Res* 62:101–5
- Kim JM, Lee H, Chang N (2002) Hyperhomocysteinemia due to short-term folate deprivation is related to electron microscopic changes in the rat brain. *J Nutr* 132:3418–21
- Kitaguchi H, Ihara M, Saiki H, Takahashi R, Tomimoto H (2007) Capillary beds are decreased in Alzheimer's disease, but not in Binswanger's disease. *Neurosci Lett* 417:128–31

- Kohl M, Lindauer U, Dirnagl U, Villringer A (1998) Separation of changes in light scattering and chromophore concentrations during cortical spreading depression in rats. *Opt Lett* 23:555–7
- Korczyński AD (2005) The underdiagnosis of the vascular contribution to dementia. *J Neurol Sci* 229–230:3–6
- LaManna JC, Chavez JC, Pichiule P (2004) Structural and functional adaptation to hypoxia in the rat brain. *J Exp Biol* 207(Pt 18):3163–9
- Lee JG, Hudetz AG, Smith JJ, Hillard CJ, Bosnjak ZJ, Kampine JP (1994) The effects of halothane and isoflurane on cerebrocortical microcirculation and autoregulation as assessed by laser-Doppler flowmetry. *Anesth Analg* 79:58–65
- Plesnila N, Putz C, Rinecker M, Wieszorrek J, Schleinkofer L, Goetz AE, Kuebler WM (2002) Measurement of absolute values of hemoglobin oxygenation in the brain of small rodents by near infrared reflection spectrophotometry. *J Neurosci Methods* 114:107–17
- Sakata YS, Grinberg OY, Grinberg S, Springett R, Swartz HM (2005) Simultaneous NIR-EPR spectroscopy of rat brain oxygenation. *Adv Exp Med Biol* 566:357–62
- Selhub J, Bagley LC, Miller J, Rosenberg IH (2000) B vitamins, homocysteine, and neurocognitive function in the elderly. *Am J Clin Nutr* 71:614S–20S
- Smielewski P, Kirkpatrick P, Minhas P, Pickard J, Czosnyka M (1995) Can cerebrovascular reactivity be measured with near-infrared spectroscopy. *Stroke* 26:2285–92
- Snowdon DA, Greiner LH, Mortimer JA, Riley KP, Greiner PA, Markesbery WR (1997) Brain infarction and the clinical expression of Alzheimer disease. The Nun Study. *JAMA* 277:813–7
- Troen A, Rosenberg I (2005) Homocysteine and cognitive function. *Semin Vasc Med* 5:209–14
- Troen AM, Chao WH, Crivello NA, D'Anci KE, Shukitt-Hale B, Smith DE, Selhub J, Rosenberg IH (2008a) Cognitive impairment in folate-deficient rats corresponds to depleted brain phosphatidylcholine and is prevented by dietary methionine without lowering plasma homocysteine. *J Nutr* 138:2502–9
- Troen AM, Shea-Budgell M, Shukitt-Hale B, Smith DE, Selhub J, Rosenberg IH (2008b) B-vitamin deficiency causes hyperhomocysteinemia and vascular cognitive impairment in mice. *Proc Natl Acad Sci USA* 105:12474–9
- Vernieri F, Tibuzzi F, Pasqualetti P, Altamura C, Palazzo P, Rossini PM, Silvestrini M (2008) Increased cerebral vasomotor reactivity in migraine with aura: an autoregulation disorder? A transcranial Doppler and near-infrared spectroscopy study. *Cephalalgia* 28:689–95
- Vovenko EP, Chuikin AE (2008) Oxygen tension in rat cerebral cortex microvessels in acute anemia. *Neurosci Behav Physiol* 38:493–500
- Xia M, Yang S, Simpkins JW, Liu H (2007) Noninvasive monitoring of estrogen effects against ischemic stroke in rats by near-infrared spectroscopy. *Appl Opt* 46:8315–21



This work is licensed under the Creative Commons Attribution-NonCommercial-No Derivative Works 3.0 Unported License. To view a copy of this license, visit <http://creativecommons.org/licenses/by-nc-nd/3.0/>

Supplementary Information accompanies the paper on the Journal of Cerebral Blood Flow & Metabolism website (<http://www.nature.com/jcbfm>)